Research on Variable-Stiffness Mechanisms of Robot Wrists for Compliant Assembling-Clamping

Kangkang Li (likangkang@nchu.edu.cn)
Nanchang Hangkong University
Pu Xing
Nanchang Hangkong University
Xu-Kun Zhang
Nanchang Hangkong University
Qing-Guo Xia
Nanchang Hangkong University

Original Article

Keywords: Variable stiffness, robot wrist, compliant robot, assembling-clamping, rigid localization

Posted Date: May 28th, 2021

DOI: https://doi.org/10.21203/rs.3.rs-540965/v1

ORIGINAL ARTICLE

Research on variable-stiffness mechanisms of robot wrists for compliant assembling-clamping

Kang-Kang Li • Pu Xing • Xu-Kun Zhang • Qing-Guo Xia

Received June xx, 201x; revised February xx, 201x; accepted March xx, 201x

Abstract: The stiffness requirements of robot wrists vary with processes during automatic assembling-clamping of robots. The precision of robots moving workpieces to operating positions in the process of rigid localization is achieved if robot wrists equip with a large stiffness. The pose errors of workpieces in the process of compliant assembling-clamping can easily be compensated if robot wrists with a low stiffness is utilized. The present compliant wrist can not meet the stiffness requirements of different processes. A robot wrist with a large stiffness variation is proposed and its mechanisms of rigid localization and compliant assembling-clamping are studied. The pose models of wrists caused by deformations are established. The influences of wrist stiffness on the deformation of itself are researched. The mechanism of modulating wrist stiffness during compliant assembling-clamping is revealed. A structure of 3-DOF (degrees of freedom) robot wrist with a stiffness variation is proposed. The wrist stiffness is changed by modulating the pretension. The influences of pretensions and geometrical parameters on the variable-stiffness characteristics and the stiffness distribution of a wrist are researched. Finally, the experiments are carried out to verify the feasibility of the wrists finishing assembling-clamping operations by modulating the stiffness.

Keywords: Variable stiffness; robot wrist; compliant robot; assembling-clamping; rigid localization

1 Introduction

The contact between end effector of traditional rigid robot and the environment is rigid. Compliance control methods are used to compensate the pose errors of robots in the assembly and clamping process [1, 2]. The compliance control methods are usually divided into active compliance method and passive compliance method [3]. The active compliance control method is to detect the contacting forces between the ends of robots and the environments by a force sensor and then adjust the pose to compensate the pose errors according to the feedback signals[4, 5]. Therefore, the positioning accuracy and force accuracy of robots for active compliance control method are required to be high.

Passive compliance method is that robot equips compliant wrists such that the end effector of robot is kept in compliant touch with environment, and the pose errors of robot can be compensated the in a passive form. Based on the scheme, a remote center compliance (RCC) compliant wrist was developed by D.E. Whitney [6]. The RCC compliant wrist uses the force and torque generated by workpieces to correct the pose deviation between assembly part and assembly body, and assist the robot to complete the assembly operation. However, the stiffness of the RCC wrist cannot be modulated according to different stiffness requirements in the processes of rigid localization and flexible assembly [7]. One of the effective ways to change the stiffness of a robot is equiping robots with mediums with a large deformation capacity such as air fluid. The way is often used to grasp light and fragile objects. Ilievski [8] developed a new type of soft robot gripper, the stiffness of the gripper can be modulated by changing air pressure injected into the gripper. Maria presented a soft pneumatic robot arm, the end effector position can be decoupled from the stiffness of the robot arm, i.e., its stiffness can be varied independently from the position of its end effector [9].

✉ Kang-Kang Li
likangkang@nchu.edu.cn

School of Aeronautic Manufacturing Engineering, Nanchang Hangkong University, Nanchang 330063, China

However, the stiffness modulated by changing air pressure is small, so the output force exerted by the grippers on objects is small. The operation is easy to fail due to its less stiffness when the gripper grabbs heavy objects or encounters large resistances [10-12]. Another way to change the stiffness of a robot is to apply variable-stiffness mechanisms. German Aerospace Center presented a manipulator in which floating spring joint (FSJ) is used as variable-stiffness mechanisms to realize the overall variable stiffness [13]. However, the maximum rotational angle of the FSJ is $\pm$ 15° [14], so the working space of the robot is limited. In addition, the four joints of the manipulator are flexible, and the inertia force transferred from each section of the manipulator to its end effector is large, then the end effector of the manipulator is difficult to control.

The compliant wrist can automatically compensate pose error of the assembling-clamping. However, the compliant wrist cannot change stiffness in a large range, so it is difficult to complete the whole assembling-clamping process. The stiffness of variable-stiffness joint can be changed by modulating pretensions [15-18], this paper aims to use variable-stiffness joint to construct a robot wrist with a large stiffness variation. The stiffness of robot wrist can be modulated in a large range to meet the different stiffness requirements of the assembling-clamping. In addition, the variable-stiffness wrist is installed at the end of the manipulator, and each joint of the manipulator is a rigid joint, so as to avoid the inertia force transferred from each section of the manipulator to its wrist.

2 Mechanisms of rigid localization and compliant assembling-clamping of variable-stiffness wrist

As seen in Fig. 1, a variable-stiffness wrist is installed between the end of a manipulator and an actuator. In the processes of moving and locating a workpiece to the target position, the variable-stiffness wrist is modulated to the maximum stiffness to realize the rigid localization of a robot, so as to reduce the deformation of the wrist caused by the gravity of an actuator and a workpiece. After the workpiece is located to the target position, the robot wrist is modulated to the minimum stiffness and become a compliant wrist in the compliant assembling-clamping process. Then the compliant wrist can automatically modulate the relative position between a workpiece and an assembly or a fixture, so as to compensate the pose error of the assembling-clamping.

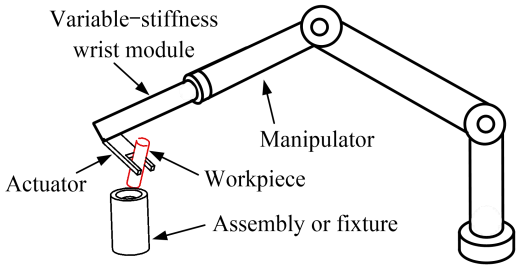

Figure 1　Manipulator with a variable-stiffness wrist

The schematic diagram of a compliant wrist assembling and clamping is shown in Fig. 2. The rolling joint, pitching joint and yawing joint of the wrist rotate around X axis, Y axis and Z axis respectively to realize the rolls, pitches and yaws of workpiece. The wrist is comprised of 3 joints connected in series, so the wrist has 3 degrees of freedom in space to realize the rotation around X axis, Y axis and Z axis. Then the poses adjusting requirements of the wrist assembling and clamping a workpiece in three-dimensional space can be meted.

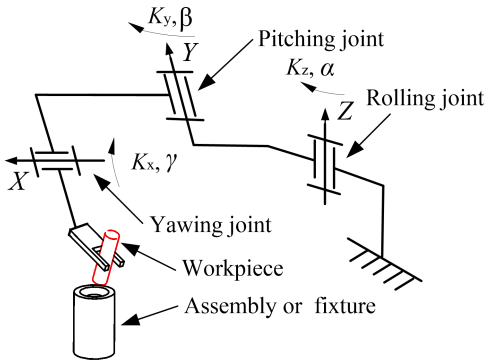

Figure 2　Schematic diagram of a compliant wrist assemblin g and clamping

3 Variable-stiffness characteristics of a robot wrist

The structure of a 3-DOF variable-stiffness wrist during rotation is shown in Fig. 3. In order to satisfy poses adjusting requirements of the wrist in three-dimensional space, the rolling joint, pitching joint and yawing joint can rotate around X axis, Y axis and Z axis respectively. The corresponding schematic diagram of a variable-stiffness wrist at the initial position is shown in Fig. 4. The lever arm O_iA_i of every variable-stiffness joint rotates around the rotating center O_i. The driving cables are connected to springs and pass through all the variable-stiffness joint. The driving cables are limited by two limiting pins at B_i point of each variable-stiffness joint. By stretching springs to modulate pretensions f_0 of the springs, the torsional stiffness rotating around X axis, Y axis and Z axis of the

wrist joint can be changed in a large range.

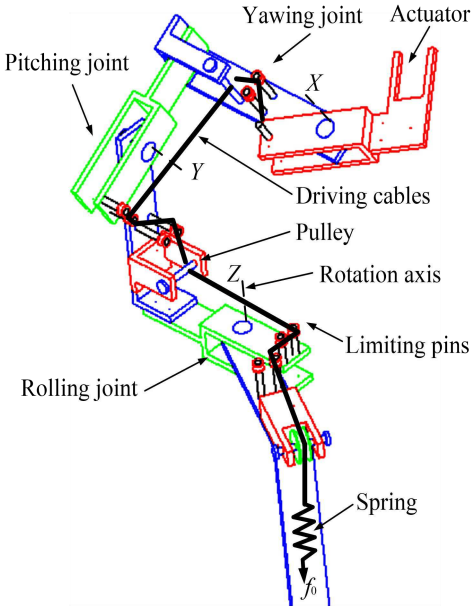

Figure 3 Structure of wrist during rotation

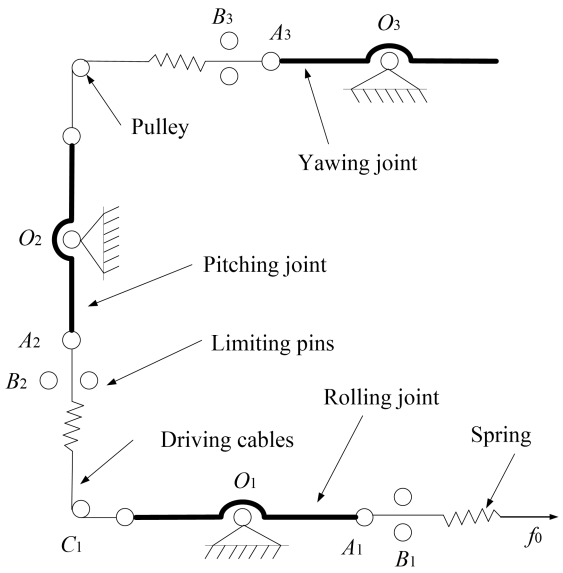

Figure 4 Schematic diagram of wrist at the initial position

As shown in Fig. 5, the wrist joint rotating around *X* axis, *Y* axis and *Z* axis respectively are three variable-stiffness joints connected in series. The driving cable is connected to a spring and pass through three variable-stiffness joint. The stiffness of the three variable-stiffness joints can be changed in a large range by modulating pretensions f_0 of the springs.

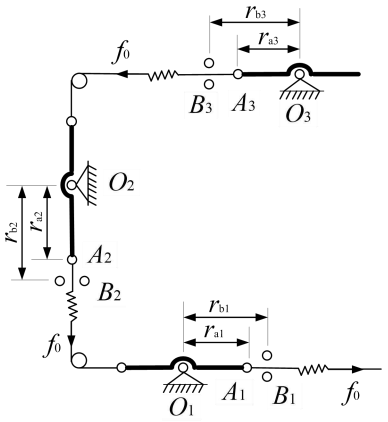

Figure 5 Schematic diagram of wrist joint

The torsional stiffness of a variable-stiffness joint is as follows [29]

$$K=f_0(r_{ai}r_{bi})/(r_{bi}-r_{ai}) \quad (1)$$

where r_{ai} is the length of the lever arm O_iA_i, r_{bi} is the distance between the rotating center O_i and the limiting point B_i, f_0 is the pretension of a spring.

It is derived from Eq.(1) that the stiffness of the joint increases with the increases of the pretension f_0 of the springs *C* linearly.

For three variable-stiffness joins, the pretension f_0 of spring are same. Therefore，their stiffness radio satisfies

$$K_1 : K_2 : K_3 = \frac{r_{a1}r_{b1}}{r_{b1}-r_{a1}} : \frac{r_{a2}r_{b2}}{r_{b2}-r_{a2}} : \frac{r_{a3}r_{b3}}{r_{b3}-r_{a3}} \quad (2)$$

It is found from Eq.(2) that the stiffness distribution of serial variable-stiffness joint are modulated by changing the geometric parameters r_{ai} and r_{bi} of each joint, and the stiffness distribution of the wrist can be kept constant in the process of modulating stiffness, so the stiffness requirements of rigid localization and compliant assembling-clamping can be met.

4 Kinematics of the variable-stiffness wrist

The motion diagram of a variable-stiffness wrist is shown in Fig. 6. The stiffness of the rolling joint is K_z. The stiffness of the pitching joint is K_y. The stiffness of the yawing joint is K_x. The spatial force $F = [F_x, F_y, F_z]^T$ is exerted on the wrist end. The frame transformation of a wrist is shown in Fig. 7. The rolling joint rotate angle, the pitching joint rotate angle and the yawing joint rotate angle are α, β and γ respectively. According to the position and the pose of wrist derived from the precision requirements of rigid localization, the rotational angles of the rolling joint, the pitching joint and the yawing joint can be obtained by the kinematics analysis of a wrist. In addition, the stiffness of the rolling joint, the pitching joint

and the yawing join can be obtained by the dynamics analysis of wrist.

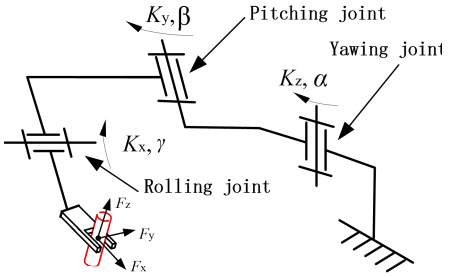

Figure 6 Motion diagram of variable-stiffness wrist

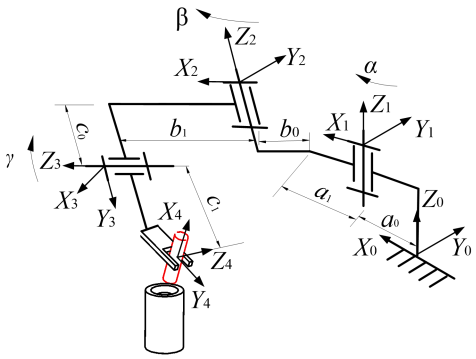

Figure 7 Frame transformation of variable-stiffness wrist

As shown in Fig. 7, starting from the inertial frame $X_0Y_0Z_0$, the reference frames for each joint are defined according to the Denavit-Hartenberg (D-H) convention. Then the transformation matrix T_4^0 from the end frame $X_4Y_4Z_4$ to the inertial frame $X_0Y_0Z_0$ is obtained by the frame transformation.

The transformation matrix $\mathbf{T}_4^0$ is expressed as [20, 21]

$$\mathbf{T}_4^0 = \mathbf{A}_1^0\mathbf{A}_2^1\mathbf{A}_4^2 \tag{3}$$

where, $\mathbf{A}_1^0$ is the transformation matrix from frame $X_1Y_1Z_1$ to frame $X_0Y_0Z_0$ of rolling joint, $\mathbf{A}_1^0 = \mathbf{Trans}(a_0,0,0)\mathbf{Rot}(Z_1,\alpha_1)$; $\mathbf{Rot}(Z_1,\alpha_1)$ is rotating transformation matrix; $\mathbf{Trans}(a_0,0,0)$ is translating transformation matrix; Similarly, $\mathbf{A}_2^1$ is the transformation matrix from frame $X_2Y_2Z_2$ to $X_1Y_1Z_1$ of pitching joint $\mathbf{A}_2^1 = \mathbf{Trans}(a_1,0,0)\mathbf{Rot}(Y_2,\text{-}90^\circ)\mathbf{Trans}(b_0,0,0)\mathbf{Rot}(Z_2,\beta_1)$; $\mathbf{A}_4^2$ is the transformation matrix from frame $X_4Y_4Z_4$ to frame $X_2Y_2Z_2$ of yawing joint, $\mathbf{A}_4^2 = \mathbf{Trans}(b_1,0,0)\mathbf{Rot}(X_4,90^\circ)\mathbf{Trans}(0,c_0,0)\mathbf{Rot}(Z_3,\gamma_1)\mathbf{Trans}(0,c_1,0)$.

The rotating transformation matrix is expressed as

$$\mathbf{Rot}(Z_1,\alpha) = \begin{bmatrix} \cos\alpha & -\sin\alpha & 0 & 0 \\ \sin\alpha & \cos\alpha & 0 & 0 \\ 0 & 0 & 1 & 0 \\ 0 & 0 & 0 & 1 \end{bmatrix} \tag{4}$$

The translating transformation matrix is expressed as

$$\mathbf{Trans}(a_0,0,0) = \begin{bmatrix} 1 & 0 & 0 & a_0 \\ 0 & 1 & 0 & 0 \\ 0 & 0 & 1 & 0 \\ 0 & 0 & 0 & 1 \end{bmatrix} \tag{5}$$

According to the precision requirements of rigid localization, the coordinates of the wrist end can be obtained from Eq. (3), and the rotational angle α of the rolling joint, the rotational angle β of the pitching joint and the rotational angle γ of the yawing joint can be obtained from Eq. (3).

The coordinate of the wrist end can be derived fro m Eq.(3) as follows

$$\begin{bmatrix} x \\ y \\ z \end{bmatrix} = \begin{bmatrix} c_0\cos\alpha - c_1\cos\alpha\cos\gamma + c_1\sin\alpha\sin\beta\sin\gamma - b_1\sin\alpha\sin\beta + a_1\cos\alpha \\ -c_1(\cos\alpha\sin\beta\sin\gamma + \sin\alpha\cos\gamma) - c_0\sin\alpha + b_1\cos\alpha\sin\beta \\ -c_1\cos\beta\sin\gamma + b_1(\cos\beta - 1) \end{bmatrix} \tag{6}$$

The torque of each joint caused by the stiffness is the product of the stiffness and the rotational angle, i. e.

$$\tau=[\tau_x\ ,\ \tau_y\ ,\ \tau_z]^T=[K_x\alpha\ ,\ K_y\beta\ ,\ K_z\gamma]^T \tag{7}$$

In addition, the torque of each joint caused by the s patial force $F = [F_x, F_y, F_z]^T$ exerted on the wrist end can be also written as follows

$$\tau=[\tau_x\ ,\ \tau_y\ ,\ \tau_z]^T=J_q^T[F_x,\ F_y,\ F_z]^T \tag{8}$$

where J_q^T is the Jacobi matrix of the wrist joints,it is the derivative of the x, y and z coordinates of the wrist end with respect to the α, β and γ rotational a ngle of the wrist joints.

Jacobi matrix of the wrist joints is expressed as

$$J_q = \begin{bmatrix} \frac{\partial x}{\partial\alpha} & \frac{\partial x}{\partial\beta} & \frac{\partial x}{\partial\gamma} \\ \frac{\partial y}{\partial\alpha} & \frac{\partial y}{\partial\beta} & \frac{\partial y}{\partial\gamma} \\ \frac{\partial z}{\partial\alpha} & \frac{\partial z}{\partial\beta} & \frac{\partial z}{\partial\gamma} \end{bmatrix} \tag{9}$$

The torque of each joint caused by the stiffness is balanced by the torque of each joint caused by the spatial force $F = [F_x, F_y, F_z]^T$ exerted on the wrist end, i.e., the Eq.(7) is equal with Eq.(8). Then the stiffness K_y of the pitching joint, the stiffness K_x of the yawing joint and the

stiffness K_z of the rolling joint can be obtained. Using the stiffness of the rolling joint, the pitching joint and the yawing joint, the length r_{ai} of the lever arm and the distance r_{bi} between the rotating center and the limiting pin of the wrist joints can be derived from Eq. (1).

5 Experiment tests on robot wrist stiffness

As shown in Fig. 8, a variable-stiffness wrist is presented. The variable-stiffness wrist is installed at the end of a manipulator, and the gripper is installed at the end of the wrist so as to grasp the workpieces. The variable-stiffness joints of the wrist are connected in series with each other. In addition, another group of symmetrical variable-stiffness joint are added to increase the wrist stiffness and balance the forces on both sides of joint. Two driving cables pass through the limiting pins of two groups of symmetrical variable-stiffness joints, they are respectively connected with two springs. The forces of two groups of symmetrical variable-stiffness joints balance each other. The other ends of two springs are connected with a motor. The pretensions are exerted on the variable-stiffness joints when the motor drives and stretches the springs. The lengths of springs can be modulated by changing the rotating angle of the motor, then the stiffness of the wrist can be modulated in a large range by changing the springs pretensions.

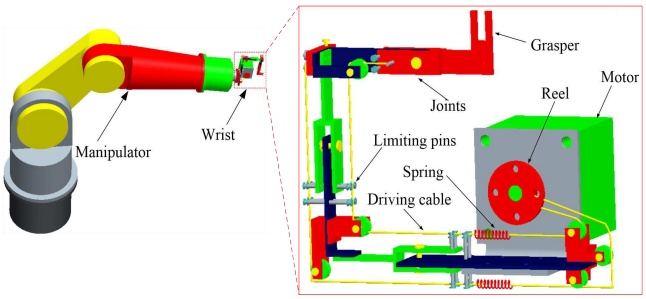

Figure 8 Structure of a variable-stiffness wrist

The experimental setups of assembling-clamping with a variable-stiffness wrist are shown in Fig. 9 and Fig. 10 respectively. A part and a workpiece are located at an assembly and a fixture by the actuator respectively at the end of the wrist in the process of rigid localization. The wrist is nearly rigid by modulating the stiffness of the wrist to a maximum value. The pose errors between a part and a hole can be compensated automatically in the following process of compliant assembling-clamping. The stiffness of the wrist is nearly to be flexible by modulating the stiffness of the wrist to be a small one according to different workpieces. The pose error between a workpiece and a chuck is compensated by the flexible wrist passively when the workpiece is clamped by a fixture. Then it can be verified that the rigid location and the compliant assembling-clamping can be realized by modulating the stiffness of the wrist in a large range.

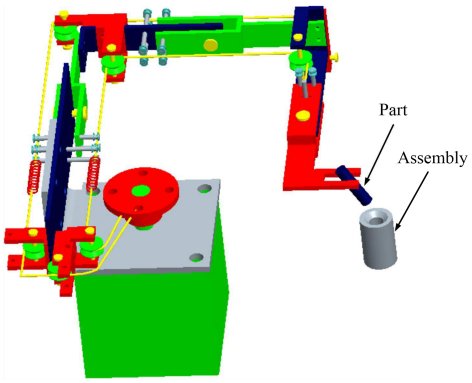

Figure 9 Experimental setups of assembling

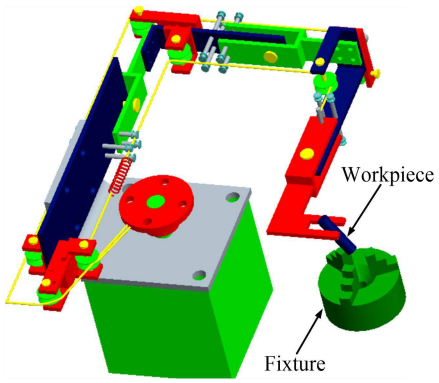

Figure 10 Experimental setups of clamping

The proposed variable-stiffness wrist is shown in Fig. 11. The yawing joint, pitching joint and rolling joint of the wrist are connected in series. Two driving cables are connected to two springs after passing through the limiting pins of two group of symmetric variable-stiffness joint. Another end of the springs are connected with a motor by cables. The springs are stretched by the motor twisting cables, then the pretensions are exerted on all the variable-stiffness joint. The springs lengths can be modulated by changing the rotating angle of the motor. Then the stiffness of the wrist can be modulated in a large range by changing the pretensions. Manipulator with the variable-stiffness wrist is shown in Fig.12, the variable-stiffness wrist is installed at the end of the manipulator by a quick pneumatic couplings.

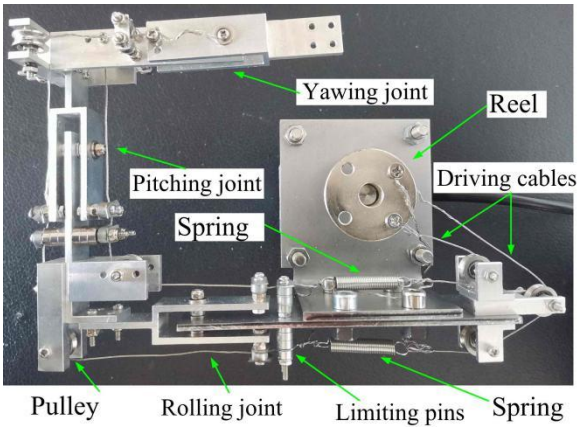

Figure 11 Prototype of a variable-stiffness wrist

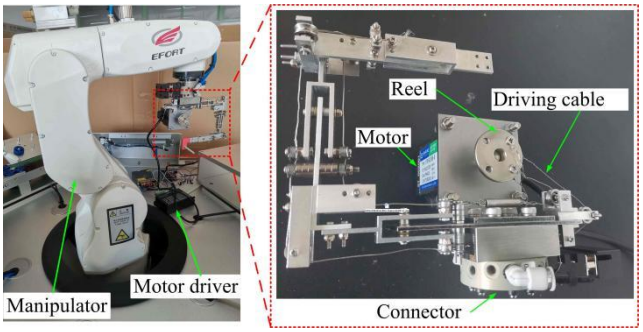

Figure 12 Manipulator with a variable-stiffness wrist

The yawing, pitching and rolling joint of the wrist are connected in series and rotate around *X* axis, *Y* axis and *Z* axis respectively. The variable-stiffness wrist has 2 groups of symmetrical variable-stiffness joint. The experimental setups of stiffness test of the yawing joint, pitching joint and rolling joint are shown in Figs.13~15, respectively. The variable-stiffness wrist is fixed on a plate, the driving cables are connected to springs, and pass through all the variable-stiffness joints. Another end of the spring is connected to a force sensor on a plate. By stretching springs to modulate pretensions of springs, the stiffness of the yawing, pitching and rolling joint of wrist can be changed. The ends of the yawing joint, pitching joint and rolling joint rotate after being exerted a load torque. A loading cable is connected to a force sensor to measure the exerted load torque. The motion images of the yawing, pitching and rolling joint are collected by a camera, the angle of each joint is measured according to the collected images. The experimental stiffness is obtained by the ratio of the load torque to the measured angle.

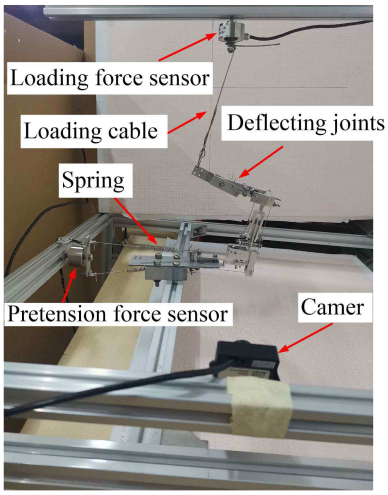

Figure 13 Stiffness test of yawing joint

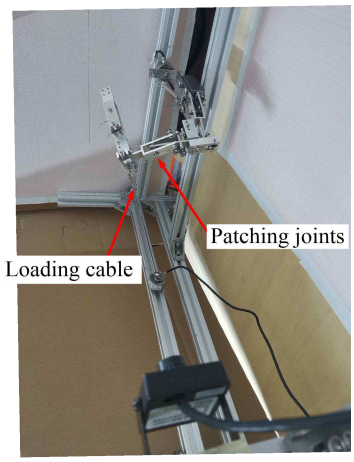

Figure 14 Stiffness test of pitching joint

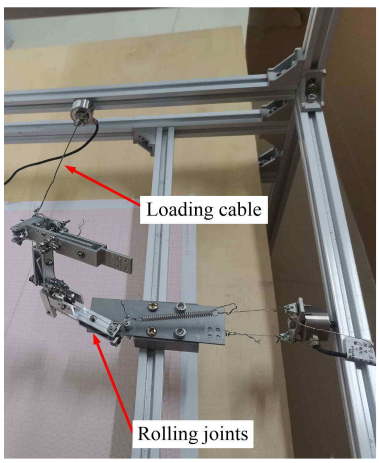

Figure 15 Stiffness test of rolling joint

For the yawing joint, pitching joint and rolling joint of wrist, the lengths of the lever arms r_a = 20 mm, the

distances between the rotating centers and the limiting points r_b = 28 mm. The stiffness variations of the rolling joint, pitching joint and yawing joint with the pretension f_0 are shown in Fig. 16. The theoretical stiffness of the rolling joint, pitching joint and yawing joint can be obtained from Eq.(1). In addition, the experimental stiffness is more than theoretical stiffness due to the friction of the experiment setup. The stiffness of the wrist increases with the increases of the pretensions of springs linearly, and the stiffness distributions of the yawing joint, pitching joint and rolling joint are kept constant.

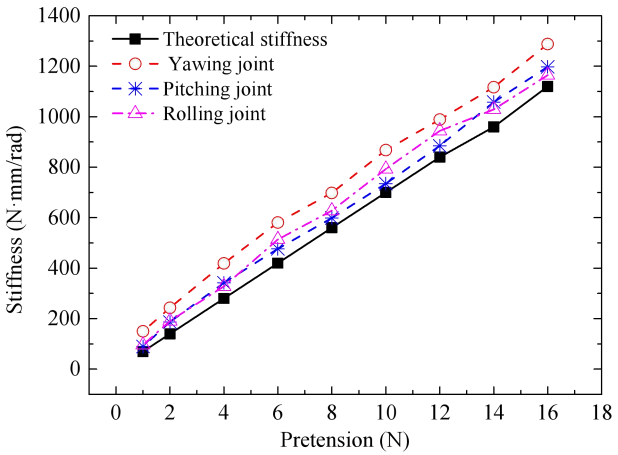

Figure 16 Wrist stiffness variations with the pretension

The assembling experiment of a variable-stiffness wrist is shown in Fig. 17. A part is assembled into the hole of an assembly by a wrist. The wrist stiffness is increased with the increase of pretensions of springs by the motor modulating the springs, then the deformation of the wrist caused by the gravity of a part is reduced, and the accuracy of locating a part to a hole is improved. The angle between the axis of the part and the axis of the hole of the assembly is 30° . In the process of compliant assembling, the wrist stiffness is decreased with the decrease of pretensions of springs by the motor modulating the springs, then the wrist become compliant. The relative pose between a part and a assembly body is modulated automatically and the pose errors between a part and a assembly body can be compensated, then the assembling process is finished.

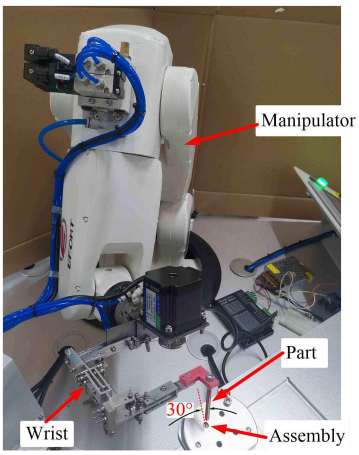

(a) Rigid location

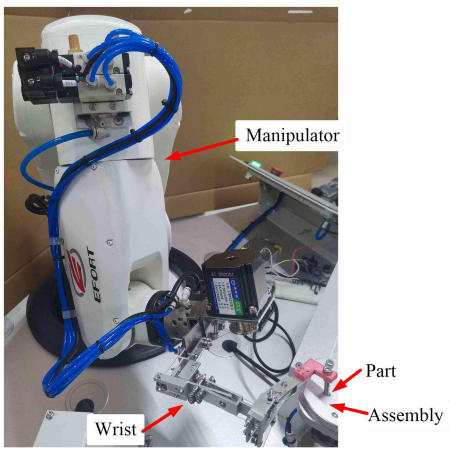

(b) Compliant assembling

Figure 17 Assembling experiment of a variable-stiffness wrist

The clamping experiment of a variable-stiffness wrist assembling is shown in Fig. 18. A workpiece is clamped into the hole of a fixture by a wrist. The wrist stiffness is increased with the increase of pretensions of springs by modulating the springs, then the deformation of the wrist caused by the gravity of a workpiece is reduced, and the accuracy of locating a workpiece to a fixture is improved. In the process of compliant clamping, the angle between the axis of workpiece and the axis of hole of the fixture is 30°. The wrist stiffness is decreased with the decrease of pretensions of springs by modulating the springs, then the wrist become compliant. The relative pose between the workpiece and the fixture is modulated automatically and the pose errors between the workpiece and the fixture can be compensated, then the clamping process is finished.

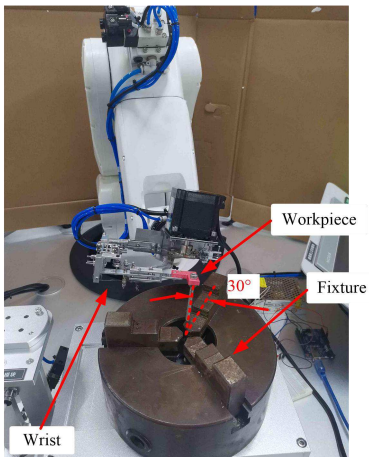

(a) Rigid location

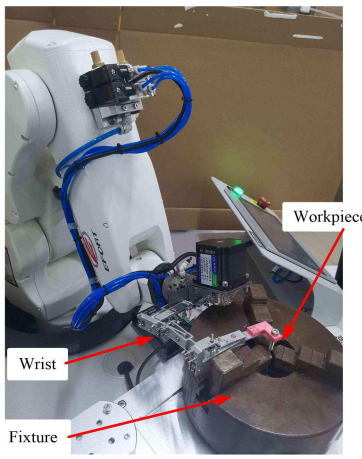

(b) Compliant clamping

Figure 18 Clamping experiment of a variable-stiffness wrist

6 Conclusions

The 3-DOF robot wrist with variable-stiffness joints is proposed to meet the stiffness requirements for different processes and different workpieces. The stiffness of wrist is modulated in a wide range by changing pretensions of springs. The stiffness of the wrist increases with the increase of pretension of springs linearly, and the stiffness distributions of wrist are kept constant. The large stiffness of robot wrists helps robots moving workpieces to operating positions with high precision in the process of rigid localizations, and the low stiffness of robot wrists is utilized to compensate the pose errors of different workpieces compliantly in the process of compliant assembling-clamping. The position and the pose of the variable-stiffness wrist are obtained by the kinematics analysis, and the stiffness of variable-stiffness joints are obtained by the dynamics analysis of wrist. The stiffness variation of the wrist with pretensions are verified by experiments, and the feasibility of the wrists finishing assembling-clamping operations by modulating the stiffness is verified by experiments.

7 Declaration

Declaration of Competing Interest

The authors declare that they have no known competing financial interests or personal relationships that could have appeared to influence the work reported in this paper.

Acknowledgement

Funding

Supported by Jiangxi Provincial Natural Science Foundation (Grant No. 20202BABL214029), National Natural Science Foundation of China (Grant No. 51868053) and National Natural Science Foundation of China(Grant No. 51768045)

Availability of data and materials

The datasets supporting the conclusions of this article are included within the article.

Authors' contributions

The author' contributions are as follows: Kang-Kang Li was in charge of the whole trial; Qing-Guo Xia wrote the manuscript; Pu Xing and Xu-Kun Zhang assisted with sampling and laboratory analyses.

Competing interests

The authors declare no competing financial interests.

Consent for publication

Not applicable

Ethics approval and consent to participate

Not applicable

References

[1] S G Nurzaman, F Iida, L Margheri, C Laschi. Soft robotics on the move: scientific networks, activities, and future challenges. *Soft Robot*, 2014; 1: 154-158.

[2] C A Nelson, L Nouaille, Gérard Poisson. A redundant rehabilitation robot with a variable stiffness mechanism, *Mech Mach Theory*, 2020; 150: 103862.

[3] S P Emmanouil, R N C Peter, S D Jian. Passivity preservation for variable impedance control of compliant robots. *IEEE/ASME Transactions on Mechatronics,* 2020; 25(5):2342-2353.

[4] J F Shi，D Q Wang, F LYan, et al. Research of the direct teaching of industrial robots based on active compliance control. *Transactions of the Chinese Society for Agricultural Machinery,* 2017; 12: 66-69. (in chinese)

[5] R Caccavale, A Finzi. Flexible task execution and attentional regulations in human-robot interaction. *IEEE Transactions on Cognitive & Developmental Systems*, 2017; 9(1): 68-79.
[6] D E Whitney, J M Rourke. Mechanical behavior and design equations for elastomer shear pad remote center compliances. *J Dyn Syst Meas Control*, 1986; 108: 223-232.
[7] D E Whitney. Historical perspective and state of the art in robot force control. *J Med Robot Res*, 1987; 6: 262-268.
[8] F Ilievski, A D Mazzeo, R F Shepherd, X Chen, G M Whitesides. Soft Robotics for Chemists. *Angew Chem*, 2015; 123: 1930-1935.
[9] M E Giannaccini, C Xiang, A Atyabi, et al. Novel Design of a Soft Lightweight Pneumatic Continuum Robot Arm with Decoupled Variable Stiffness and Positioning. *Soft Robot*, 2018; 5: 54-70.
[10] G Zhong, Y Hou, W Dou. A soft pneumatic dexterous gripper with convertible grasping modes. *Int J Mech Sci*, 2019; 153: 445-456.
[11] H Huang, J Lin, L Wu, et al. Optimal control scheme for pneumatic soft actuator under comparison of proportional and PWM-solenoid valves. *Photonic Netw Commun*, 2019; 37: 153-163.
[12] J H Yan, P P Shi, X B Zhang, et al. Review of Biomimetic Mechanism, Actuation, Modeling and Control in Soft Manipulators. *Chin J Mech Eng*, 2018; 54: 1-14.
[13] M Grebenstein, M Chalon, W Friedl, et al. The hand of the DLR Hand Arm System: Designed for interaction. *Int J Rob Res*, 2012; 31: 1531-1555.
[14] E Oliver, H Sami, W Michael. On joint design with intrinsic variable compliance: derivation of the DLR QA-joint. *2010 IEEE International Conference on Robotics and Automation*, *May 3-8, 2010, Anchorage, Alaska, USA*, 2010. p. 1687-1694.
[15] N I Tsagarakis, C D G Sardellitti. A new variable stiffness actuator (CompAct-VSA): design and modelling. *Proceedings of the 2011 IEEE/RSJ International Conference on Intelligent Robots and Systems, September 25-30, 2011, San Francisco, CA, USA*, 2011. p. 378-383
[16] R Van Ham, B Vanderborght, M Van Damme, et al. MACCEPA, the mechanically adjustable compliance and controllable equilibrium position actuator: Design and implementation in a biped robot. *Rob Auton Syst,* 2007; 55: 761-768.
[17] B Vanderborght, N G Tsagarakis, R Van Ham, et al. MACCEPA 2.0: compliant actuator used for energy efficient hopping robot Chobino1D. *Auton Robots*, 2011; 31: 55-65.
[18] D Chakarov. Optimization synthesis of parallel manipulators with desired stiffness. *J Theor App Mech*, 1998; 4: 18-31.
[19] K K Li, H Z Jiang, S Y Wang, et al. A soft robotic fish with variable-stiffness decoupled mechanisms. *J Bionic Eng,* 2018; 15: 599-609.
[20] M Shimizu. Analytical inverse kinematics for 5-DOF humanoid manipulator under arbitrarily specified unconstrained orientation of end-effector. *Robotica*, 2015; 33: 1-21.
[21] W Xu, L Yan, Z Mu, et al. Dual arm-angle parameterisation and its applications for analytical inverse kinematics of redundant manipulators. *Robotica*,2016; 34: 2669-2688.

Figures

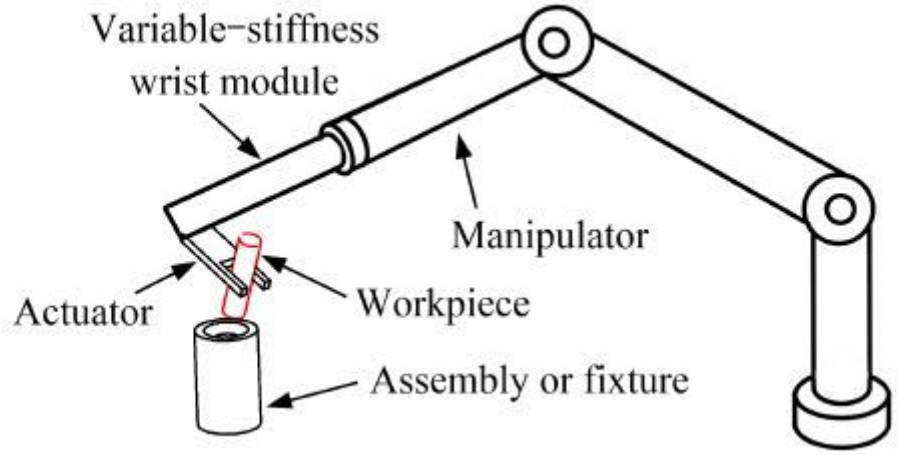

Figure 1

Manipulator with a variable-stiffness wrist

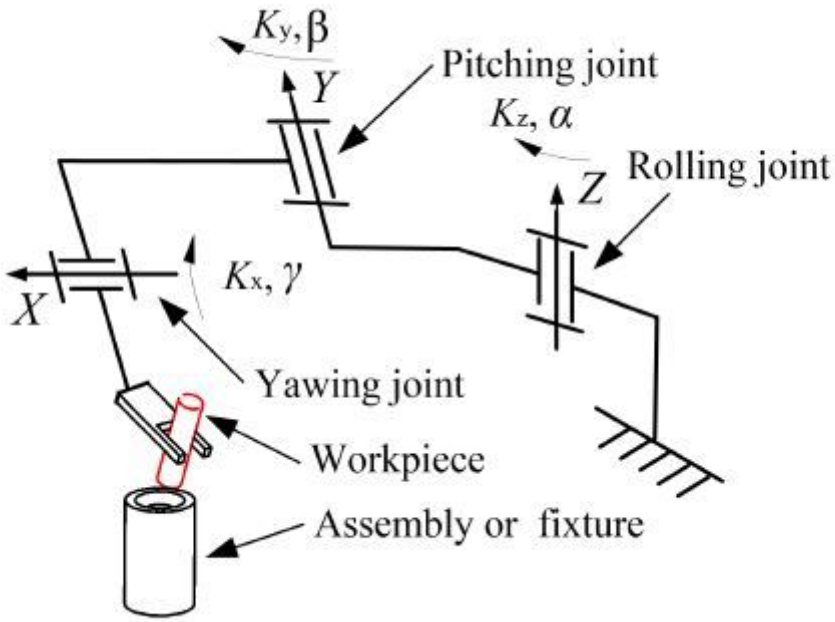

Figure 2

Schematic diagram of a compliant wrist assembling and clamping

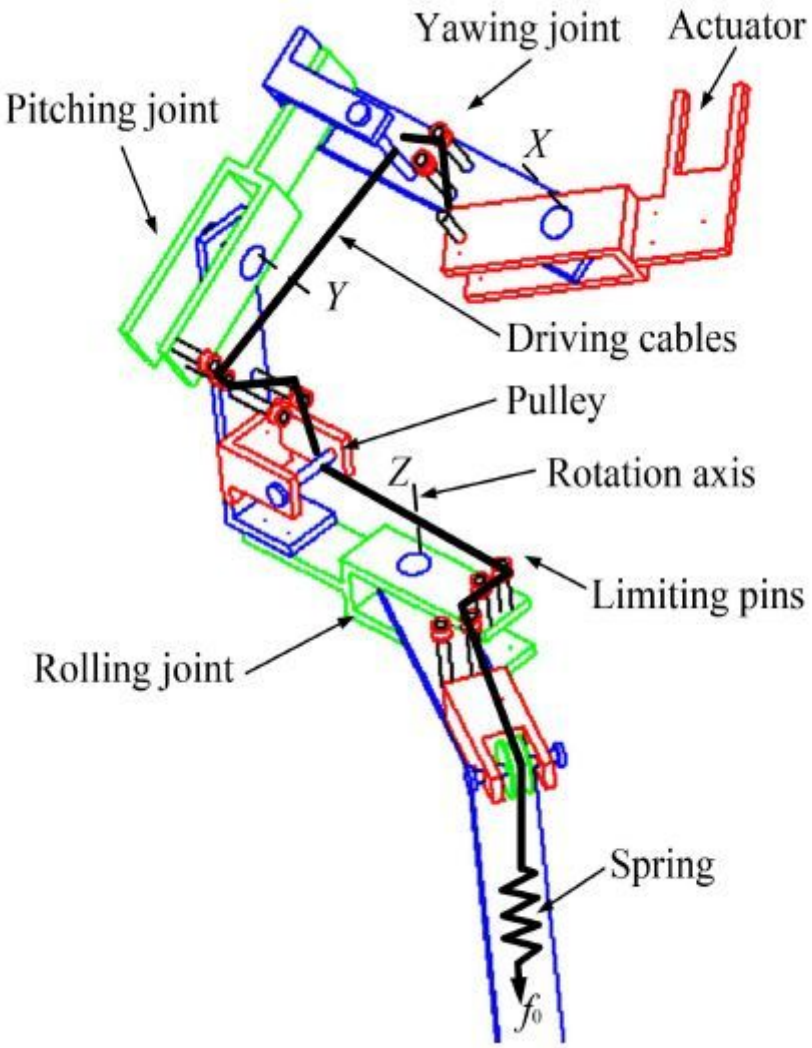

Figure 3

Structure of wrist during rotation

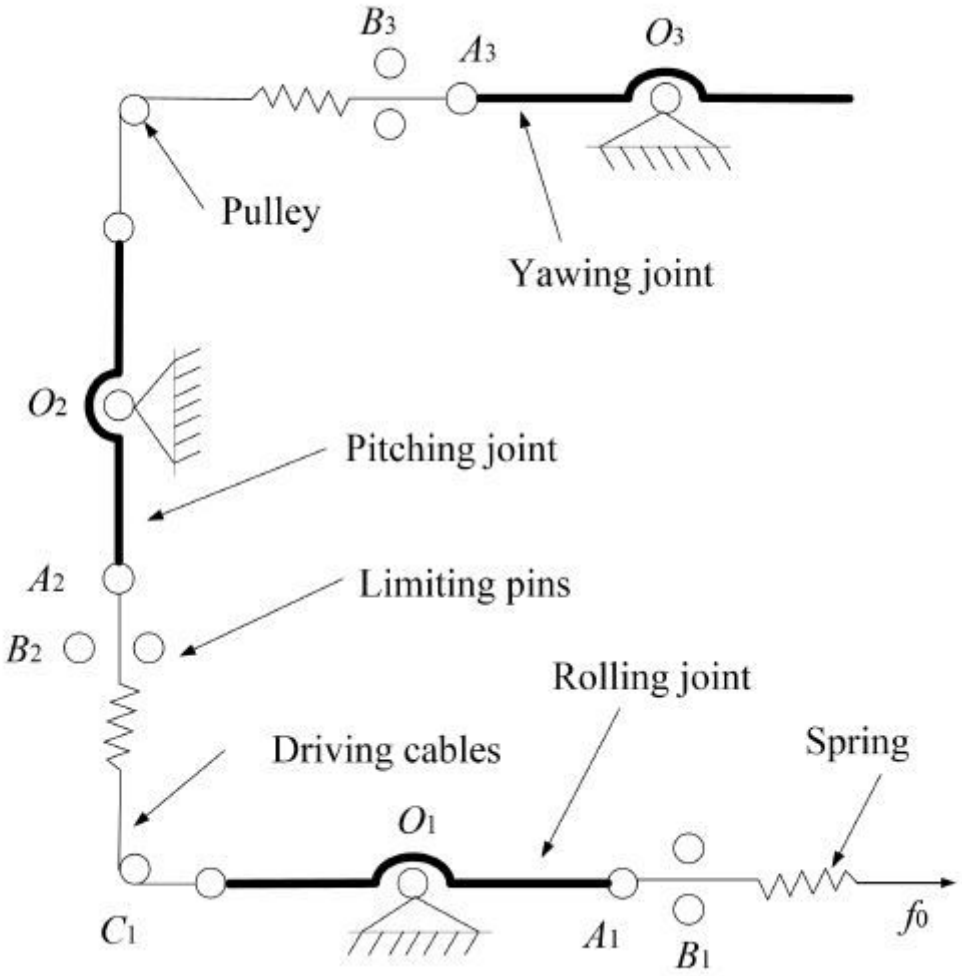

Figure 4

Schematic diagram of wrist at the initial position

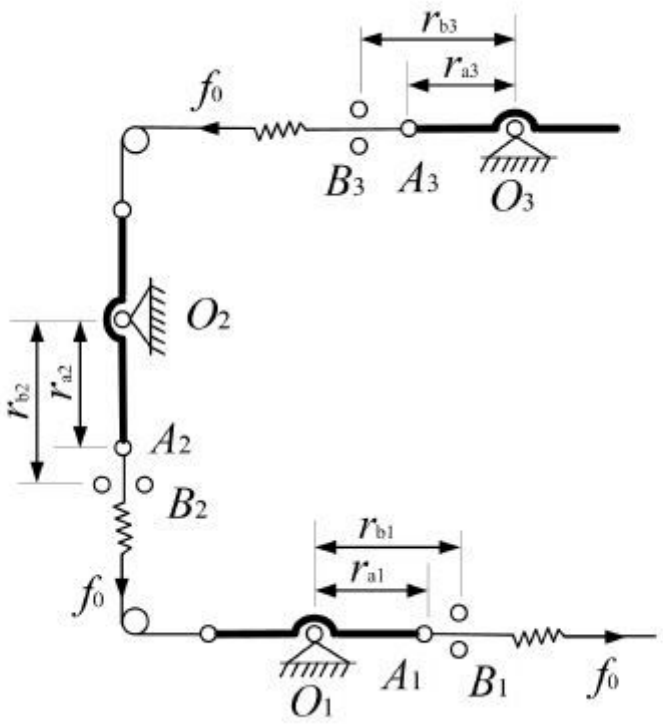

Figure 5

Schematic diagram of wrist joint

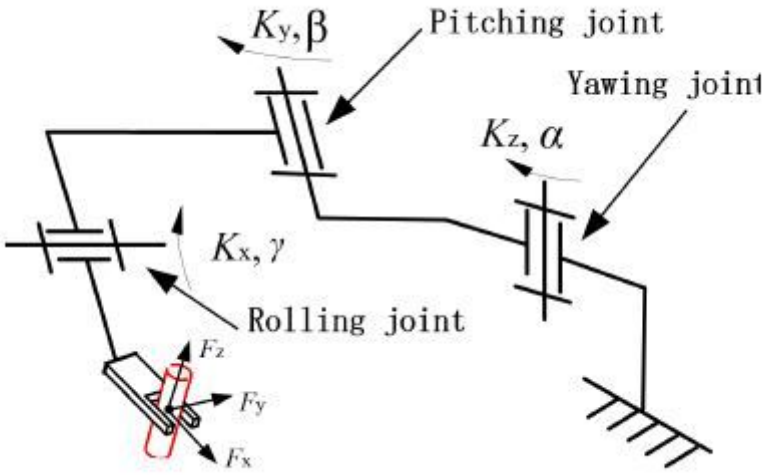

Figure 6

Motion diagram of variable-stiffness wrist

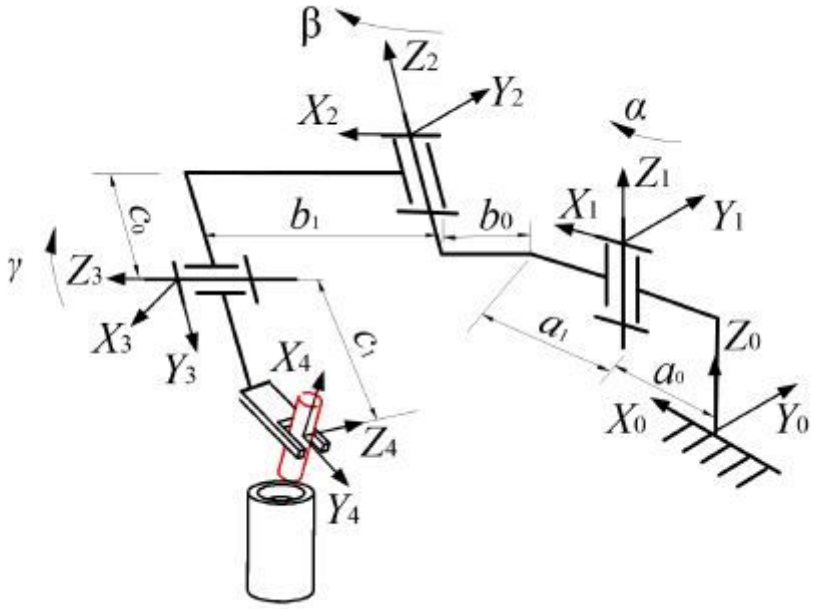

Figure 7

Frame transformation of variable-stiffness wrist

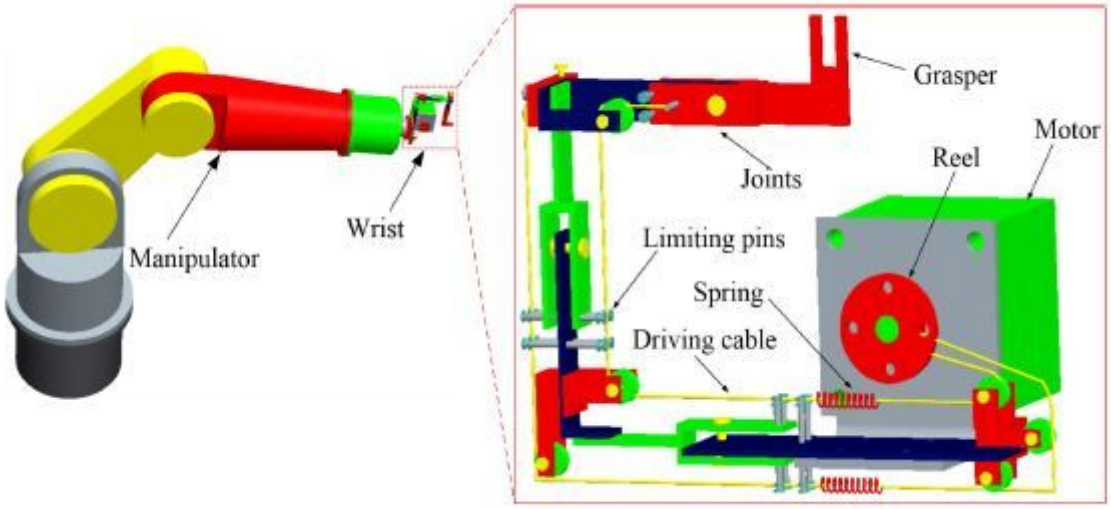

Figure 8

Structure of a variable-stiffness wrist

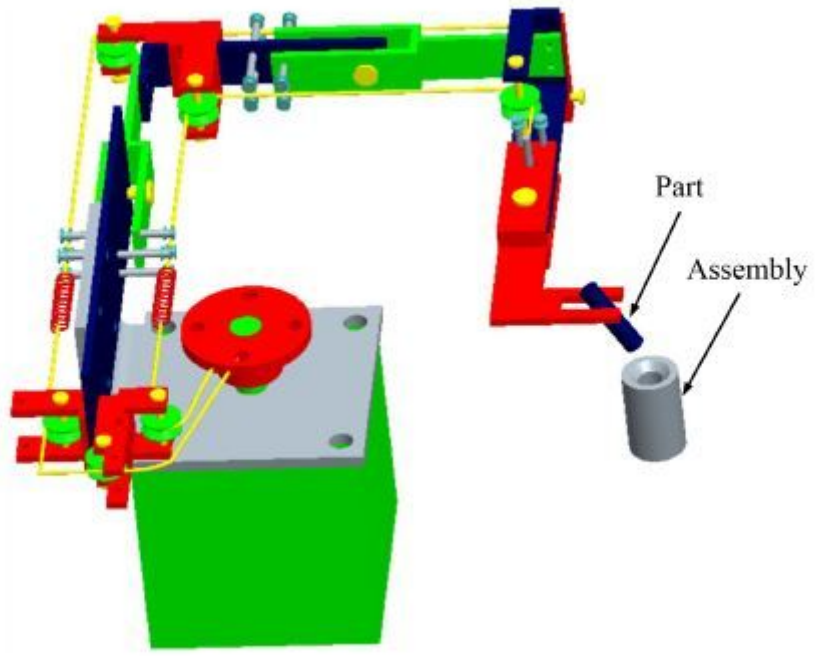

Figure 9

Experimental setups of assembling

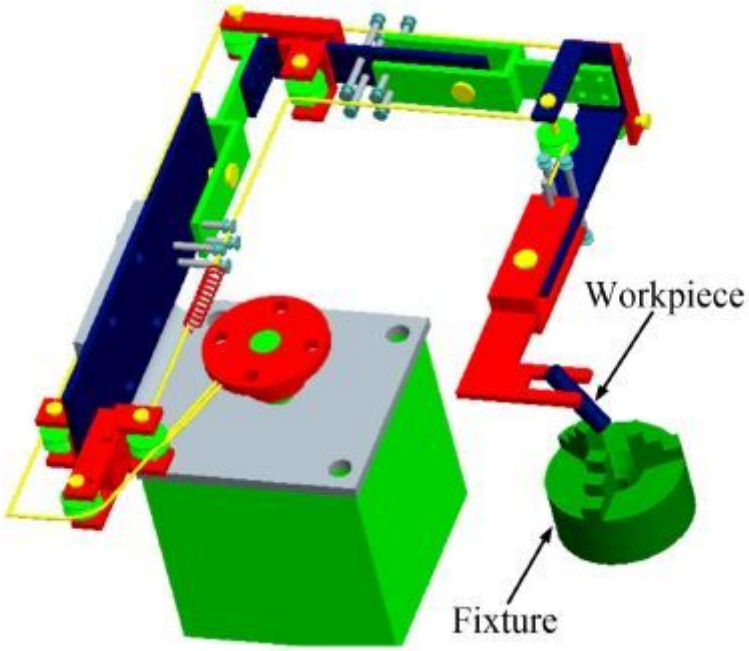

Figure 10

Experimental setups of clamping

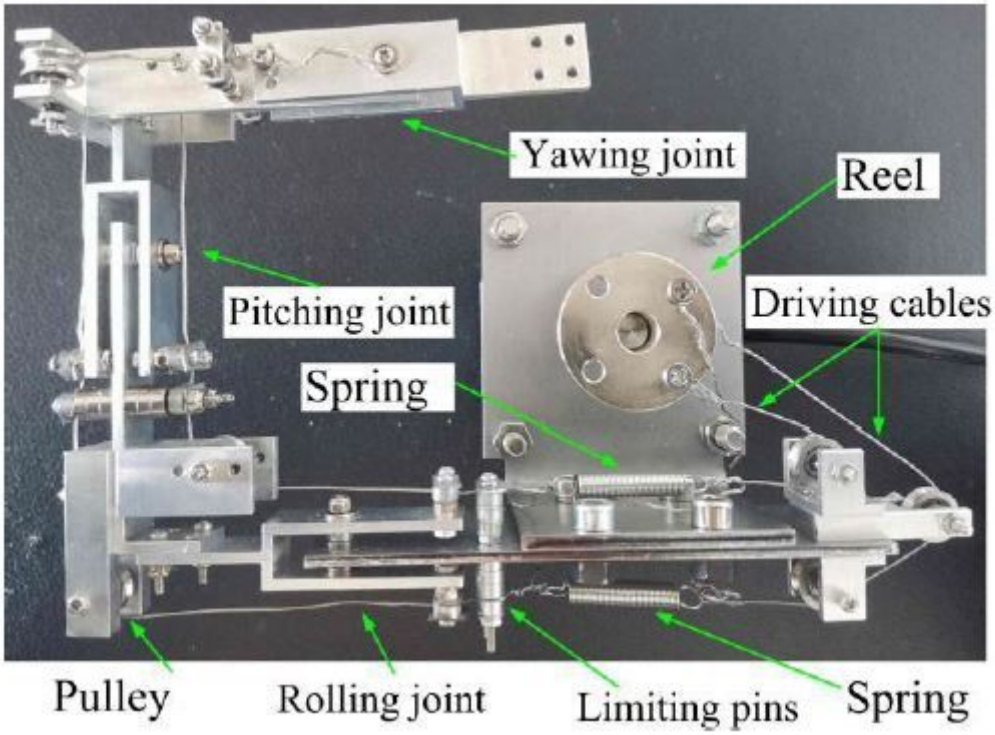

Figure 11

Prototype of a variable-stiffness wrist

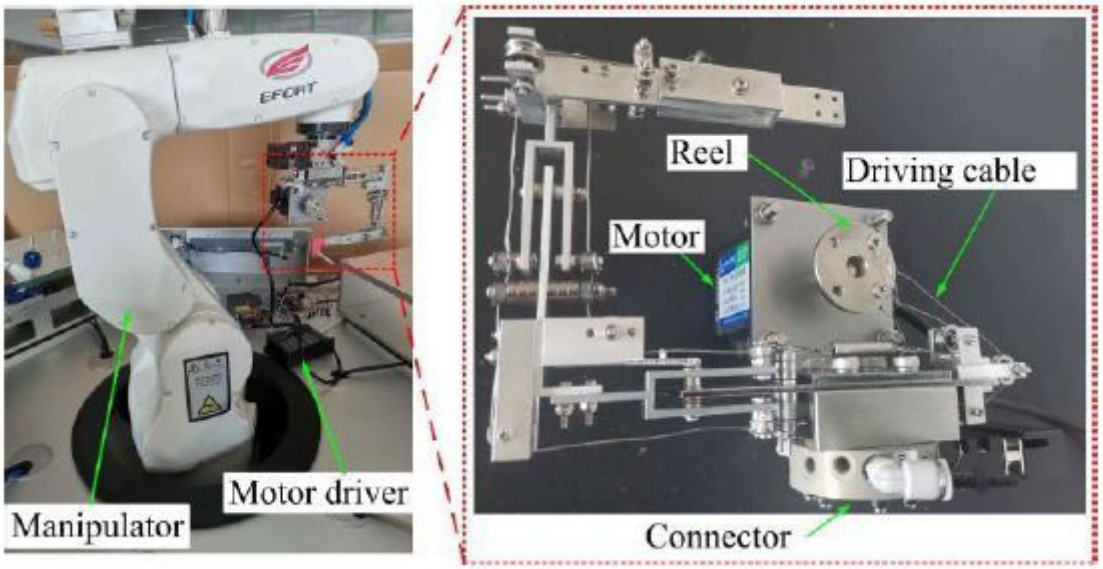

Figure 12

Manipulator with a variable-stiffness wrist

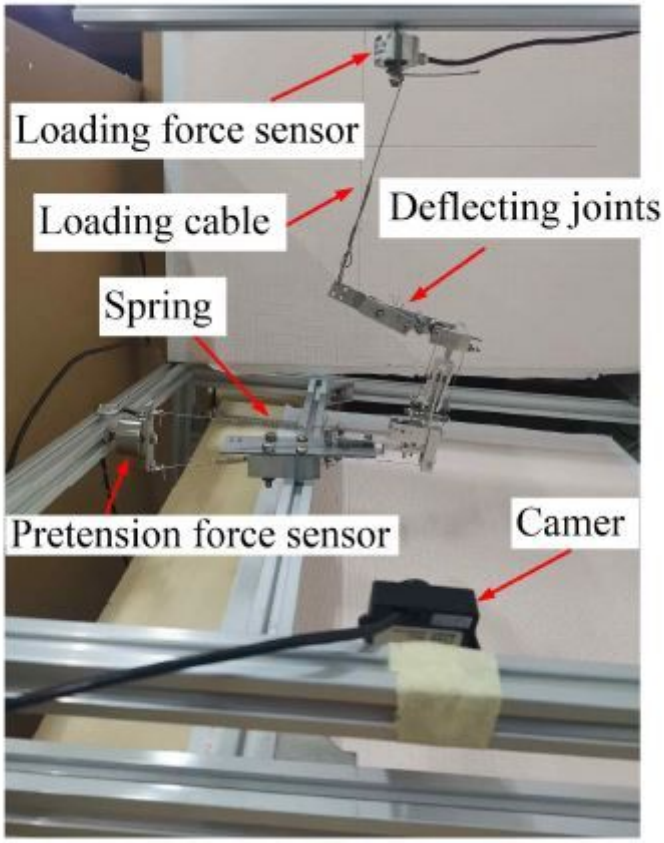

Figure 13

Stiffness test of yawing joint

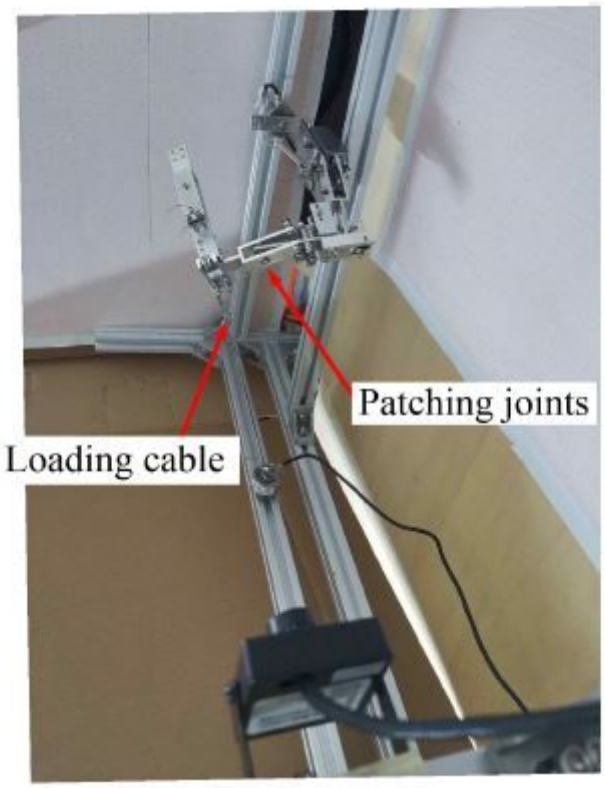

Figure 14

Stiffness test of pitching joint

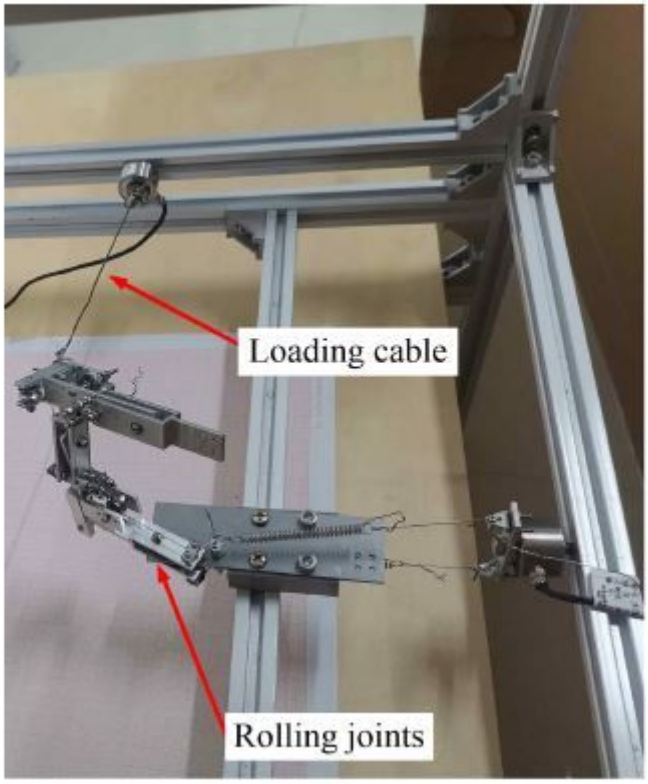

Figure 15

Stiffness test of rolling joint

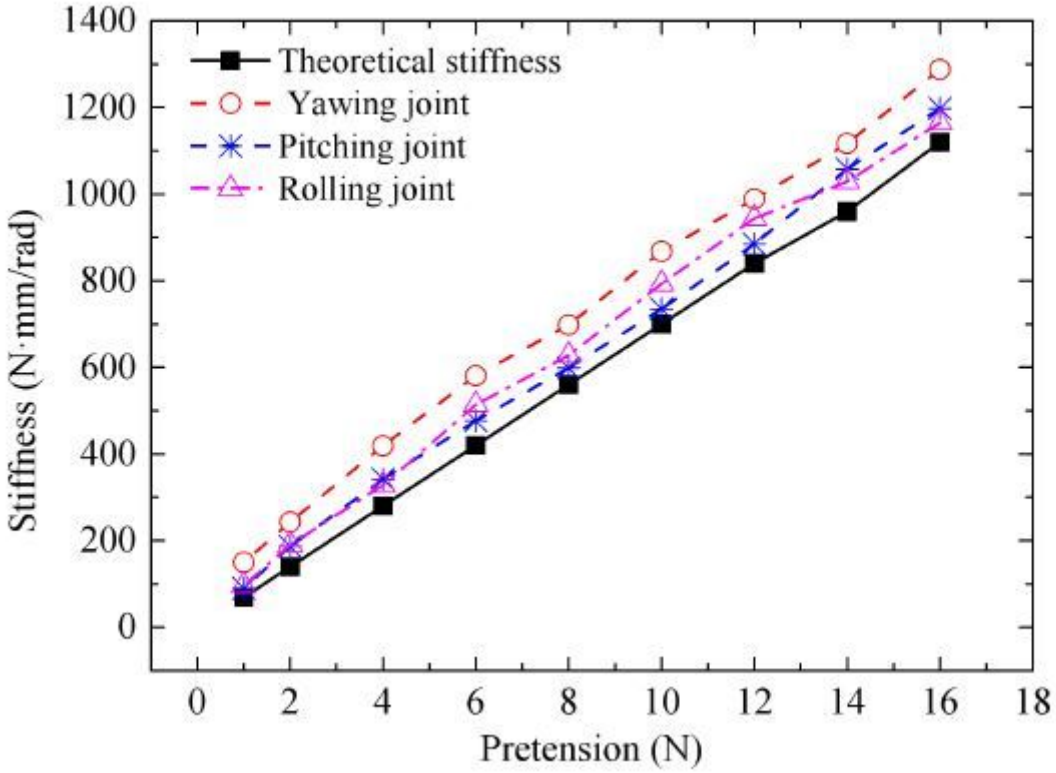

Figure 16

Wrist stiffness variations with the pretension

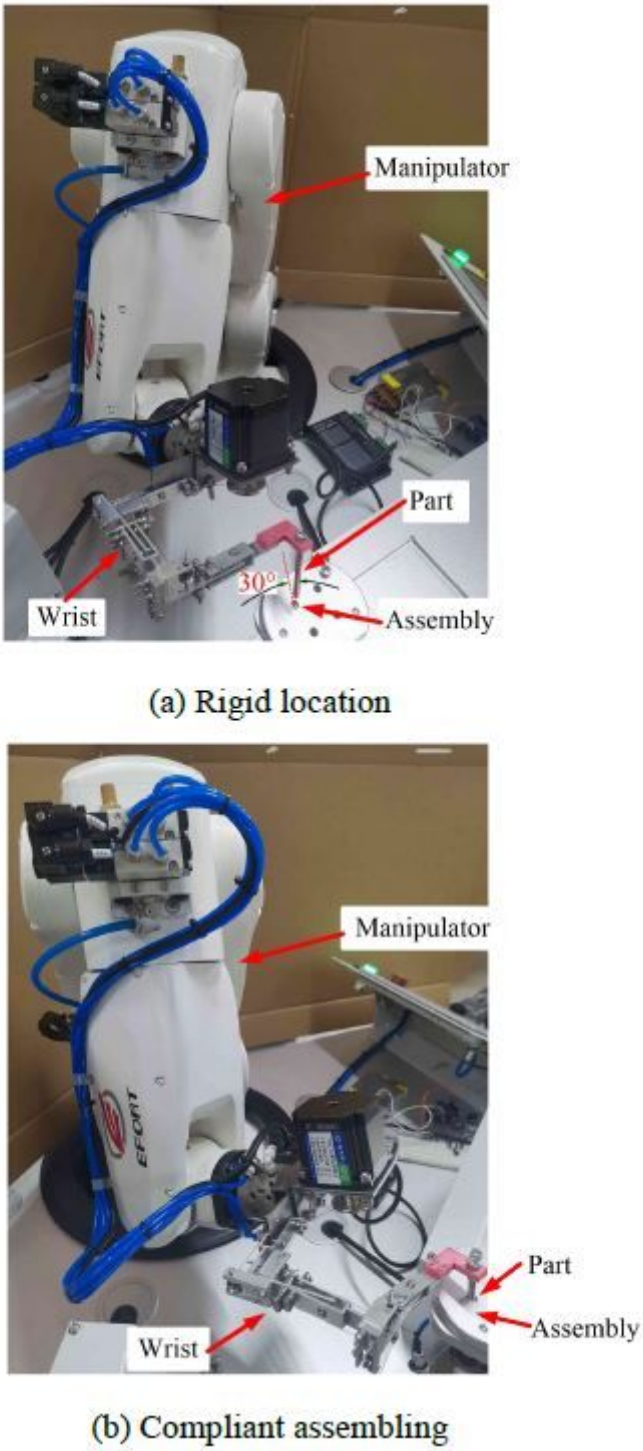

Figure 17

Assembling experiment of a variable-stiffness wrist

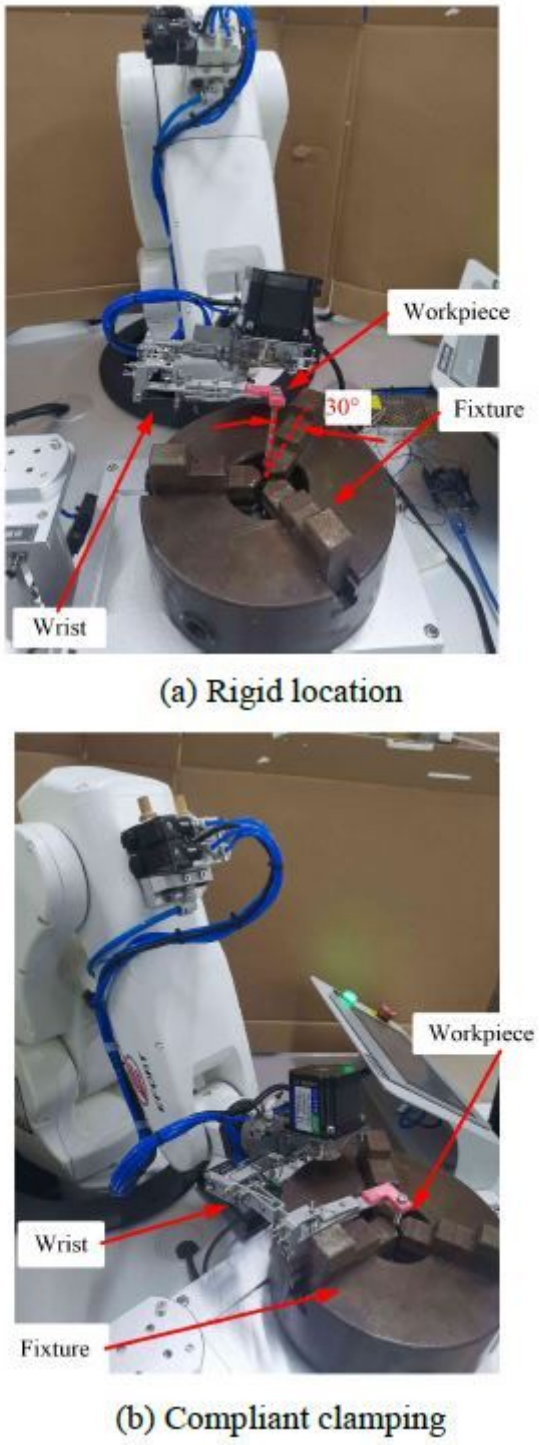

Figure 18

Clamping experiment of a variable-stiffness wrist